Hybrid Quantum Chemical and Density Functional Theory (ONIOM) Study of the Acid Sites in Zeolite ZSM-5

Kaido Sillar and Peeter Burk*

Institute of Chemical Physics, University of Tartu, 2 Jakobi Street, 51014 Tartu, Estonia

Received: December 9, 2003; In Final Form: May 4, 2004

The three-layer ONIOM(B3LYP/6-311+G**:HF/3-21G*:MNDO) method was used to model the structural, energetic, and spectroscopic (IR and ^{1}H NMR) properties of the acid sites (types 1 and 2) of zeolite ZSM-5. The calculation method used reproduced the properties of studied acid sites well. In the case of the second type of Brønsted acid site, the hydrogen of the bridged hydroxyl group forms a hydrogen bond with the next nearest oxygen to the aluminum atom. The analysis of experimental IR and ^{1}H NMR spectra in combination with current calculations suggests that the experimentally observable mean acidity of zeolite ZSM-5 depends on temperature because the occupancies of protons at various oxygen sites are kinetically controlled and thermodynamic equilibrium is reached at high temperatures.

1. Introduction

Zeolite ZSM-5 is an important shape-selective solid acid catalyst. It is used in the petrochemical industry for the catalytic cracking of hydrocarbons (FCC additive) and the conversion of methanol to gasoline (MTG process). Also, processes such as the production of ethylbenzene by alkylation of benzene, xylene isomerization, and toluene disproportionation run over ZSM-5-containing catalysts.[1]

Catalytically active centers in zeolites are bridged hydroxyl groups (Si−O(H)−Al) that act as strong Brønsted acid sites. Information about the properties of these hydroxyl groups in zeolites is obtained experimentally with IR and NMR spectroscopic measurements. Two types of bridged hydroxyl groups are identified in zeolite ZSM-5. In addition to a well-known peak at ca. 3610 cm^{-1} (type 1)[2] in the IR spectrum of zeolite ZSM-5, Zholobenko et al.[3] reported the existence of a relatively broad IR band at ca. 3250 cm^{-1} (type 2) and assigned it to a "complex with a hydrogen bond between acidic OH groups and one of the neighboring oxygen atoms in the zeolitic lattice". Also, several ^{1}H MAS NMR studies have shown two different types of Brønsted acid sites in zeolite ZSM-5, namely, free bridging hydroxyl groups (line b at ca. 4.2 ppm, type 1) and bridging hydroxyl groups influenced by an additional interaction with the zeolitic framework (line b′ at ca. 7 ppm, type 2).[4−7] The later peak is visible as a broad shoulder on the downfield side of the main peak at 4.2 ppm in many previously measured ^{1}H MAS NMR spectra of zeolite ZSM-5.[8−12] This shoulder sharpens into a clearly resolved peak when the temperature is reduced to 123 K,[4] which could be explained by a chemical exchange that is frozen at low temperatures.[6] On the basis of the experimental data described above, Freude[6] proposed a model where the hydrogen atom of the second type of bridged hydroxyl group can jump between two or more of the four oxygen atoms around one aluminum atom, and one of these positions is affected by additional electrostatic interaction with other framework oxygens.

Valuable information about energetic, structural, and spectroscopic properties of the Brønsted acid sites can be obtained from quantum chemical modeling of hydroxyl groups in zeolites. High-level electron correlation methods and flexible basis sets are needed for the quantitative prediction of interactions that are weaker than covalent bonding (hydrogen-bonded systems, intramolecular interactions) or NMR chemical shifts. Zeolites may have several hundred atoms per unit cell, which makes the use of these sophisticated methods computationally very expensive. Modeling active sites of zeolites with relatively small clusters makes it possible to use high-level quantum chemistry methods, but clusters are treated like molecules in the gas phase and therefore they neglect long-range interactions (electrostatic effects) and structure constrains of the periodic solid.[13−16] Consequently, the cluster approach cannot discriminate between acid sites in different crystallographic positions or frameworks. Full relaxation of clusters may also lead to structures that do not resemble acid sites in real zeolitic lattices.[17]

Lattice effects are often implicitly included in calculations by using experimental zeolite structures with only partial geometry optimization.[18−20] However, Sauer et al.[13] have pointed out that because the local geometry of zeolites acid sites is not precisely known fixing some geometry parameters may cause artificial strain. Another possible approach is to use hybrid (QM/MM) methods, which have been developed for the calculation of large systems. In the case of hybrid methods, the large molecules are divided into layers, where a chemically important part (active site) is treated at a high level of theory and the rest of the system is described by a computationally less-demanding method. Sauer et al. have successfully used the QM-Pot scheme in the investigation of zeolites, and to our knowledge, only they have computationally studied the second type of bridging hydroxyl groups in zeolite ZSM-5.[15] The ONIOM method,[21−23] developed by Morokuma and co-workers, is a more general hybrid method, which can combine any number of molecular orbital as well as molecular mechanics, methods, and it is reported to be an efficient tool for accurately calculating NMR chemical shifts[24] and weak chemical interactions[25] in large systems. We previously[26] tested the performance of the ONIOM method to reproduce the properties of the acid sites of zeolite ZSM-5 and found that the ONIOM method can differentiate between crystallographically different acid sites. Also, the studies of zeolites ZSM-5 and TS-1 using the ONIOM

* Corresponding author. Tel: +372-7-375-258. Fax: +372-7-375-264. E-mail: peeter@chem.ut.ee.

10.1021/jp037770s CCC: $27.50
Published on Web 06/18/2004

TABLE 1: Calculated Geometry Parameters of the Bridged Hydroxyl Groups Formed around Aluminum at the T6 Site[a]

	Al6−O6−Si2		Al6−O19−Si3		Al6−O5−Si5	Al6−O18−Si9
	free	H bonded	H bonded	H bonded	free	free
O−H	0.9703	0.9955	0.9881	0.9882	0.9741	0.9721
OH···O	2.3251[b]	1.7828[c]	1.8368[d]	1.8810[e]	2.1516[b]	2.2286[f]
Al−O(H)	1.9766	1.9577	1.9511	1.9704	1.9196	1.9137
Si−O(H)	1.7117	1.7061	1.7082	1.7111	1.6935	1.6918
Al−O−H	101.06	103.96	107.64	104.52	99.72	102.28
Si−O−H	115.77	117.00	109.70	116.87	115.20	116.88
O−Al−O(H)	90.42	95.46	95.68	95.96	87.41	88.84
Al−O(H)−Si	142.66	136.36	141.24	137.86	144.73	140.83

[a] Bond lengths in angstroms, bond angles in deg. [b] Distance to O18. [c] Distance to O4, [d] Distance to O11. [e] Distance to O8. [f] Distance to O5.

TABLE 2: Calculated Geometry Parameters of the Bridged Hydroxyl Groups Formed around Aluminum at the T7 Site[a]

	Al7−O17−Si4	Al7−O7−Si8	Al7−O23−Si7		Al7−O22−Si11
	free	free	free	H bonded	H bonded
O−H	0.9710	0.9695	0.9714	0.9966	0.9977
OH···O	2.2833[b]	2.4398[c]	2.2217[d]	1.7747[e]	1.7622[d]
Al−O(H)	1.9578	1.9266	1.9612	1.9484	1.9211
Si−O(H)	1.6987	1.7060	1.6952	1.6903	1.6902
Al−O−H	102.32	106.27	100.26	104.72	106.06
Si−O−H	114.64	115.06	117.51	119.15	119.88
O−Al−O(H)	89.24	93.40	88.02	95.06	96.23
Al−O(H)−Si	138.55	138.53	142.00	134.65	132.66

[a] Bond lengths in angstroms, bond angles in deg. [b] Distance to O23. [c] Distance to O17. [d] Distance to O22. [e] Distance to O7.

method[27−30] have shown that lattice effects could be included in ONIOM method calculations and that they have a significant effect on calculated structural, energetic, and spectroscopic properties.

In the current work, we use the ONIOM method to model the properties of the acid sites of zeolite ZSM-5. Our primary goal is to characterize the second type of Brønsted acid sites, that is, to describe the properties of bridged hydroxyl groups that are influenced by additional electrostatic interaction with the zeolite framework.

2. Computational Details

Definition of Cluster. In the orthorhombic form of zeolite ZSM-5, there are 12 crystallographically distinct tetrahedral sites (T sites) occupied by Si or Al atoms.[31] There is no experimental information about the preferred position of aluminum atoms in the zeolite's lattice. In the current work, two different aluminum atom locations (at the T6 and the T7 sites) were chosen, and all four acid sites that form when protons are attached to one of the oxygen atoms bonded directly to the aluminum atom were studied. Thus, the present study covers acid sites in eight crystallographically different positions. (For details, see Tables 1 and 2.)

In ONIOM calculations, the molecular system, which is divided into layers or parts, is called the real system. The most important part of the molecule (reaction center) is called the model system and is described at the highest level of theory. In the two-layered ONIOM method, the total energy of the system is obtained from three independent calculations:

$$E^{\mathrm{ONIOM2}} = E^{\mathrm{high}}_{\mathrm{model\ system}} + E^{\mathrm{low}}_{\mathrm{real\ system}} - E^{\mathrm{low}}_{\mathrm{model\ system}} \quad (1)$$

The ONIOM method can be viewed as an extrapolation scheme. Starting from $E^{\mathrm{low}}_{\mathrm{model\ system}}$, the extrapolation to the high-level calculation ($E^{\mathrm{high}}_{\mathrm{model\ system}} - E^{\mathrm{low}}_{\mathrm{model\ system}}$) and the extrapolation to the real system ($E^{\mathrm{low}}_{\mathrm{real\ system}} - E^{\mathrm{low}}_{\mathrm{model\ system}}$) are assumed to give an estimate for $E^{\mathrm{high}}_{\mathrm{real\ system}}$. In the case of the three-layered ONIOM method, the ONIOM energy is defined according to eq 2.

$$E^{\mathrm{ONIOM3}} = E^{\mathrm{high}}_{\mathrm{model\ system}} + E^{\mathrm{medium}}_{\mathrm{middle\ system}} - E^{\mathrm{medium}}_{\mathrm{model\ system}} + E^{\mathrm{low}}_{\mathrm{real\ system}} - E^{\mathrm{low}}_{\mathrm{middle\ system}} \quad (2)$$

All acid sites have been modeled by the three-layer ONIOM method using clusters (the real system) consisting of 108 T atoms (1 Al and 107 Si atoms). It might be argued that the cluster incorporating 108 T atoms is still too small to mimic the interactions (especially electrostatics) within the full periodic zeolite structure. However, the inclusion of another shell of T atoms even at the lowest level would have been too demanding for our computational resources. It should also be noted that in our current model the farthest atoms in the cluster are ca. 8.5 Å away from the hydroxyl group so that the atoms of the next shell would be even farther from the site of interest. We propose that the electrostatic interaction with atoms that far away (unaccounted for in the current model) can be considered to be a small, constant systematic error that does not influence our conclusions.

The high-level model system part includes two complete coordination shells of T atoms around the central hydroxyl group (8T model, $(H_3SiO)_3-Si(OH)Al-(OSiH_3)_3$), or using the notation from ref 17, the high-level model system is represented by the {SiO(H)Al}shell-2 model. The middle system, treated at the medium level of theory, enfolds another complete shell of T atoms around the high-level model system. Again using the notation from ref 17, the dimensions of the middle system extend to the size of the {SiO(H)Al}shell-4 model (Figure 1). Hydrogen atoms are used as link atoms and to saturate the dangling bonds of the whole cluster (real system). The distances corresponding to the bonds between link atoms (hydrogens) and silicon atoms in the model system are defined to be proportional to Si−O distances in the real system (standard proportionality factor $g = r(\mathrm{Si-H})/r(\mathrm{Si-O}) = 0.862$ is used in Gaussian 98[32]). It has been demonstrated[33] that the ONIOM energies and optimized geometries do not depend on that factor, except for clearly unreasonable values of g.

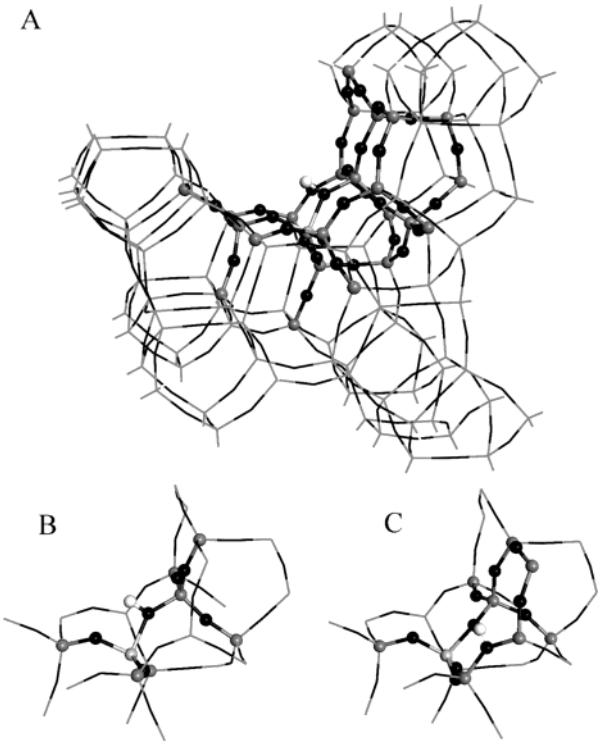

Figure 1. Illustration of the partitioning schemes used in the case of the Al7−O7(H)−Si8 acid site. The used cluster (real system) with high- and medium-level parts is shown in ball-and-stick style (A). The first type of bridged hydroxyl group calculated with the 8T-size model system (ball-and-stick style) surrounded by the middle system is shown in line style (B). The second type of bridged hydroxyl group calculated with extended-size model system (ball-and-stick style) surrounded by the middle system is shown in line style (C).

Morokuma et al.[24] have pointed out that the model system should extend over all atoms that are directly bonded to the atoms of interest. Therefore, the clusters, modeling of hydroxyl groups involved in hydrogen bonding, are calculated additionally with an alternative partitioning scheme, where the model system is extended at the expense of the middle system to cover complete rings involved in H-bond formation (Figure 1C).

Computational Methods. All calculations were performed using the standard implementation of the ONIOM method in the Gaussian 98[32] program package. Full geometry optimizations were carried out with the ONIOM(B3LYP/6-311+G**:HF/3-21G*:MNDO) method for all clusters studied. To locate the bridged hydroxyl groups of the second type, we used different starting geometries in the case of each acid site.

We have shown[26] that using the MNDO method in the calculation of the energies of low-level real system results in energies that have a systematic erroneous contribution to the ONIOM deprotonation energies of zeolites. To avoid this inaccuracy, we chose to omit the MNDO contribution from ONIOM3 energies and to use only high- and medium-level energies from the ONIOM3 calculations. Therefore, the energetic properties that we used are extrapolated only from energies calculated at high and medium level (ONIOM2(B3LYP/6-311+G**:HF/3-21G*)) and are named ONIOM2 energies. Deprotonation energies were calculated as ONIOM2 energy changes of reaction 1 (at 0 K).

$$ZH \rightleftharpoons Z^- + H^+ \qquad (3)$$

The absolute deprotonation energies cannot, of course, be measured experimentally. However, absolute deprotonation energies are useful for comparison with the molecular gas-phase superacids and for the prediction of the catalytic properties. They also provide, albeit somewhat artificial, anchoring points for experimentally measured relative acidities.

SCHEME 1: Schematic Representation of the Hydrogen Bond Formation in Case of the Second Type of Brønsted Acid Site

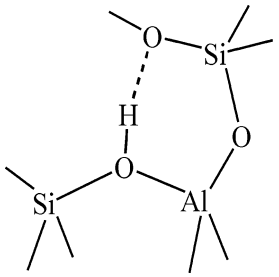

Experimental[34,35] and computational studies[36−38] have shown that the O−H stretching mode is essentially a pure mode; that is, it is uncoupled from all other vibrations of the zeolite framework, and therefore the bridging hydroxyls can be treated as isolated diatomic fragments, O−H. Meijer et al. have recently shown[39] that in the case of strong hydrogen bonding with adsorbed base the stretch−bend interactions might be considerable. Still, we have, in the current work, assumed that for the studied systems with relatively weak hydrogen bonding the bridging hydroxyl can be treated as an isolated diatomic fragment. Because the standard frequency calculations were prohibitively expensive for us and we are mainly interested in stretching vibrational frequencies of bridged hydroxyl groups, the anharmonic stretching vibrational frequencies of bridged hydroxyl groups were estimated as follows. A series of single-point calculations were performed at various fixed O−H bond lengths whereas other atoms were kept fixed in their equilibrium positions. The O−H bond lengths were varied by ±0.25 Å from the equilibrium bond length in steps of 0.05 Å. The obtained potential energy surface was fit to the Morse function from which the anharmonicity constant and vibrational frequencies were determined.[40,41] This approach has shown good results in previous studies of modeling OH vibrations in zeolites.[36,40,41]

^{1}H NMR chemical shifts have been evaluated from the isotropic absolute (chemical) shielding constants σ obtained according to formula 2 using gauge-including atomic orbitals (GIAO).

$$\sigma^{\text{ONIOM2(B3LYP/6-311+G**:HF/3-21G*)}} = \sigma^{\text{B3LYP/6-311+G**}}_{\text{model system}} + \sigma^{\text{HF/3-21G*}}_{\text{middle system}} - \sigma^{\text{HF/3-21G*}}_{\text{model system}} \qquad (4)$$

For a reference, tetramethylsilane, computed at the B3LYP/6-311+G** level of theory (σ_{TMS} = 31.98 ppm), was used.

3. Results and Discussion

Both types of bridged hydroxyl groups (types 1 and 2) are represented among the studied acid sites (shown in Figure 1). In the case of the second type of Brønsted acid site, the hydrogen of the bridged hydroxyl group forms a hydrogen bond with the next nearest oxygen to the aluminum atom (Scheme 1).

Tables 1 and 2 present a selection of calculated geometry parameters of the bridged hydroxyl groups in studied crystallographic positions. The lengths of the calculated hydrogen bonds are between 1.7622 and 1.8810 Å, where the hydrogen bonds in five-membered rings (Al6−O6(H)−Si2 and Al6−O19-(H)−Si3 sites) are somewhat longer than those in six-membered

SCHEME 2: Schematic Representation of an Electrostatic Interaction between Hydrogen Atom in the First Type of Bridged Hydroxyl Group and Nearest Oxygen of Zeolites Framework

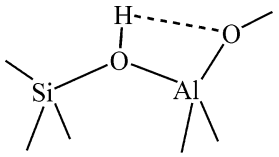

SCHEME 3: Schematic Representation of Used Clusters for Quantitative Estimation of the Electrostatic Interaction between Hydrogen in Bridged Hydroxyl Group and Nearby Oxygen

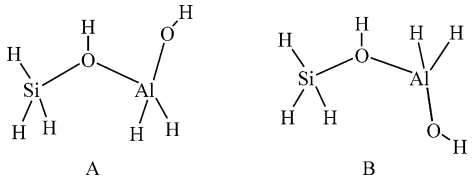

rings (Al7−O7(H)−Si8 and Al7−O22(H)−S11 sites). The O−H bond lengths of hydroxyl groups, which are influenced by a hydrogen bond, are about 0.02 Å longer than those in free hydroxyl groups.

In protonated (neutral) zeolites, the comparison of bond lengths and bond angles associated with the aluminum atom shows that the Al−O(H) bond lengths are about 0.2 Å longer than Al−O(Si) bonds and that O−Al−O(H) bond angles are decreased by 8.4° on average, compared to those for the anionic form, whereas O−Al−O bond angles are increased by 6.9°, resulting in an average O−Al−O bond angle of 116.5°. This distortion of the local environment around Al toward a slightly trigonal coordination has also been reported previously by other computational studies,[20,42−44] and it was used to explain the line broadening and the large quadrupole coupling constant in the ^{27}Al NMR spectra of dehydrated H zeolites.[44,45]

The distances from hydrogen (in the first type of bridged hydroxyl group, see Scheme 2) to the nearest oxygen (bonded to aluminum) are quite small, ranging from 2.1516 to 2.4398 Å. The comparison of O−Al−O(H) angles at different Al centers shows that the angles involving oxygens nearest to the hydroxyl groups' hydrogens are also about 17° smaller than the rest of the O−Al−O(H) angles. In our opinion, those contracted O−Al−O(H) angles (average bond angle is 89.6°) and small Al−O−H angles (an average bond angle is 102.0°) are most likely caused by the electrostatic interaction between hydrogen in the first type of bridged hydroxyl group and the nearby framework oxygen (Scheme 2).

For the quantitative estimation of the strength of that electrostatic interaction, additional calculations were performed with small clusters presented in Scheme 3.

The energy difference between fully optimized (at B3LYP/6-311+G** level of theory) conformers A and B (from Scheme 3) is 1.3 kcal/mol (1 kcal/mol = 4.184 kJ/mol); thus, the energy of that interaction is small but definitely not negligible.

The geometries, calculated for the clusters with the extended model system, are very similar to those that are calculated with the 8T-size model system (Table 3). The effect of the inclusion of the electron correlation on all atoms involved in hydrogen bonding can be witnessed by somewhat decreased O−H bond lengths and up to 0.3-Å increased hydrogen bond lengths. As a result, the second type of hydroxyl group in the Al6−O19−Si3 site (with the hydrogen bond to O11) changes to the first type of hydroxyl group (closest oxygen to the hydroxyl hydrogen is O5).

TABLE 3: Geometry Parameters of the Second Type of Bridged Hydroxyl Groups Calculated on Clusters with the Extended Model System[a]

	Al6−O6−Si2	Al6−O19−Si3		Al7−O7−Si8	Al7−O22−Si11
O−H	0.9826	0.9760	0.9771	0.9831	0.9843
OH···O	1.9869[b]	2.1590[c]	2.1810[d]	1.9981[e]	1.9565[f]
Al−O(H)	1.9641	1.9692	1.9765	1.9560	1.9279
Si−O(H)	1.7109	1.7083	1.7161	1.6958	1.6960
Al−O−H	104.41	97.15	104.60	105.95	107.67
Si−O−H	114.06	113.44	113.77	116.16	116.69
O−Al−O(H)	96.22	87.71	96.02	95.50	97.15
Al−O(H)−Si	139.35	148.12	141.46	136.42	134.22

[a] Bond lengths in angstroms, bond angles in deg. [b] Distance to O4. [c] Distance to O5 (distance to O11 is 2.5043 Å). [d] Distance toO8. [e] Distance to O7. [f] Distance to O22.

TABLE 4: Calculated Deprotonation Energies (DPE, in kcal/mol), ^{1}H NMR Chemical Shifts (δ, in ppm), and Stretching Vibrational Frequencies (ω, in cm^{-1}) of Studied Bridged Hydroxyl Groups Formed around Aluminum at the T6 Site

	Al6−O6−Si2		Al6−O19−Si3		Al6−O5−Si5	Al6−O18−Si9
	free	H bonded	H bonded[a]	H bonded[b]	free	free
DPE	290.0	294.3	289.6	292.8	291.6	292.4
DPE[c]	289.7	291.9	289.6	289.8		
δ(OH)	3.9	7.3	6.7	6.4	5.2	4.9
δ(OH)[c]	3.8	6.3	5.1	5.2		
ω(OH)	3615	2897	3124	3104	3550	3588
ω(OH)[c]	3626	3291	3512	3432		

[a] Hydrogen bond with O11; in the case of clusters calculated with the extended model system, the second type of bridged hydroxyl group is changed to the first type of bridged hydroxyl group, where the closest oxygen to the hydroxyl hydrogen is O5. [b] Hydrogen bond to O8. [c] Calculated using clusters with the extended model system

TABLE 5: Calculated Deprotonation Energies (DPE, in kcal/mol), ^{1}H NMR Chemical Shifts (δ, in ppm), and Stretching Vibrational Frequencies (ω, in cm^{-1}) of Studied Bridged Hydroxyl Groups Formed around Aluminum at the T7 Site

	Al7−O17−Si4	Al7−O23−Si7	Al7−O7−Si8		Al7−O22−Si11
	free	free	free	H bonded	H bonded
DPE	290.9	290.8	290.5	295.6	296.9
DPE[a]			290.5	292.5	294.5
δ(OH)	4.2	4.3	4.5	7.7	8.0
δ(OH)[a]			4.4	6.5	7.0
ω(OH)	3608	3639	3587	2847	2829
ω(OH)[a]			3592	3273	3248

[a] Calculated using clusters with the extended model system.

Calculated deprotonation energies of the studied hydroxyl groups (Tables 4 and 5) are in good accordance with experimental estimations[46] and previous theoretical studies[13,15,20,26] of zeolite ZSM-5. From the comparison of the deprotonation energies of hydroxyl groups in different crystallographic positions, estimations of the relative stabilities of different acid sites can be made. The larger the deprotonation energy, the harder it is to detach a proton from the zeolite's framework, and thus, the proton for a given T site is expected to be located on the oxygen with the greatest deprotonation energy. In both studied aluminum sites, the calculated deprotonation energies of the second type of bridged hydroxyl groups are the highest as upon

deprotonation; therefore, additional energy is needed to break the hydrogen bonds. This is also evidenced by low-temperature ^{1}H MAS NMR investigations of the interactions between surface hydroxyl groups and CO molecules,[7] where at low coverage only the signal from the first type of bridged hydroxyl groups is affected by adsorbed CO in contrast to the signal from the second type of bridged hydroxyl groups that remain unperturbed.

The strength of hydrogen bonds can be estimated from the comparison of the deprotonation energies of free and hydrogen-bonded bridged hydroxyl groups in same crystallographic positions. Obtained hydrogen bond energies are 4.3 and 5.1 kcal/mol for Al6−O6−Si2 and Al7−O7−Si8 sites, respectively.

The deprotonation energies calculated for the clusters with the extended model system are up to 3.1 kcal/mol lower than those calculated for the clusters with the 8T-size model system. The weakening of hydrogen bonds (hydrogen bond energies are 1.9 and 2.0 kcal/mol for Al6−O6−Si2 and Al7−O7−Si8 sites respectively) after the inclusion of the electron correlation in all atoms involved in hydrogen bonding is consistent with the increase in hydrogen bond length by analogous comparison.

To the best of our knowledge, only Zholobenko et al.[3] and Brunner et al.[5] have used infrared spectroscopy in the investigation of the second type of bridged hydroxyl groups. They have reported the existence of a broad adsorption band, characteristic of hydrogen-bonded systems, centered at about 3250 cm^{-1} in IR spectra of zeolite ZSM-5. Our estimated vibrational frequencies of hydrogen-bonded hydroxyl groups calculated on clusters with the 8T-size model system range from 2829 to 3124 cm^{-1}; frequencies calculated for clusters with the extended model system are about 400 cm^{-1} higher and, as a result, are in better agreement with experimental measurements. The calculated stretching frequency (3432 cm^{-1}) of the hydroxyl group in the Al6−O19−Si3 site with a hydrogen bond to O8 is approximately 160 cm^{-1} higher compared to that of the other three OH groups involved in hydrogen bonding (with frequencies ranging from 3248 to 3291 cm^{-1}). This can be explained by the comparative weakness of that hydrogen bond, which is also evidenced by the longest hydrogen-bond length and small deprotonation energy.

The stretching vibrational frequencies of free bridged hydroxyl groups are characterized by an infrared absorption band at 3610 cm^{-1} in infrared spectra of zeolite ZSM-5. The latter band is split into three submaxima at 3606, 3619, and 3627 cm^{-1} by lowering the temperature to 170 K, and after exchanging hydroxyl protons with deuterium, two additional submaxima are revealed.[2] Furthermore, in steamed zeolite ZSM-5, Datka et al.[47] reported the existence of very strongly acidic hydroxyl groups characterized by an IR band at 3590 cm^{-1}. Our estimated vibrational frequencies are in good agreement with those experimental findings; that is, different IR absorption submaxima are well reproduced by our ONIOM calculations.

Datka et al.[2] explained the splitting of the peak at 3610 cm^{-1} into several submaxima by the heterogeneity of the OH groups, which in turn can be explained by the presence of $(SiO)_3$−Si−O(H)−Al$(OSi)_3$ groups with various bridge geometries and thus with different acid strengths. Our calculations show that acid sites formed in different crystallographic positions have different bridge geometries and deprotonation energies, but in the case of the first type of bridged hydroxyl groups, no straight correlation between Al−O(H)−Si angles and deprotonation energies can be found. This indicates that DPE is determined not just by a single (geometry) parameter but by the sum of several factors.

TABLE 6: Collection of Experimental Data from Different Measurements of ^{1}H NMR Chemical Shifts (in ppm) of Both Types of Bridged Hydroxyl Groups

type 1	type 2	reference
4.3	6.9	4
4.2	ca. 7	5
4.18 ± 0.05[a]	6.1 ± 0.1[b]	6
4.3 ± 0.2	6.5 ± 0.5	48, 49
4.2[c]	5.4[d]	50
3.9	5.9	51
4.0	6.4	52

[a] fwhm = 0.8 ± 0.1. [b] fwhm = 2.7 ± 0.3. [c] width 0.9. [d] width 2.9.

The collection of experimental data from different measurements of ^{1}H NMR chemical shifts of both types of bridged hydroxyl groups is presented in Table 6.

The deconvolution of the ^{1}H MAS NMR spectra of zeolite ZSM-5 has revealed an additional submaximum at 4.9 ppm with a small contribution to the overall spectrum.[51] This peak was assigned[51] to water molecules adsorbed at Lewis acid sites on the basis of the work of Hunger et al.[53] But originally, in ref 53, the peak from water molecules adsorbed on Lewis acid sites at low coverage was reported to be at 6.5 ppm. The comparison of experimentally measured (Table 6) and calculated ^{1}H NMR chemical shifts of both types of bridged hydroxyl groups shows that ^{1}H NMR chemical shifts of both types of bridged hydroxyl groups calculated with the ONIOM method are well in the range of the experimental findings. Thus, on the basis of our calculations, we propose that the ^{1}H NMR peak around 5.0 ppm can be assigned to the bridging hydroxyl groups.

It is shown experimentally that at room temperature the residual line width for the signals of the first type of Brønsted acid sites in ^{1}H MAS NMR spectra of evacuated zeolite catalysts is about 0.8 ppm and that the line width is determined by the distribution width of the isotropic values of the chemical shift, which in turn is explained by structural differences of the bridging hydroxyl groups.[7,8,54] The distribution of calculated ^{1}H NMR chemical shifts of the first type of bridged hydroxyl groups is somewhat wider (the distribution range is 1.3 ppm, from 3.9 to 5.2 ppm) than experimentally determined, probably because all sites do not get populated at moderate temperatures as discussed below.

The shape of the absorption bands, in both IR and ^{1}H NMR spectra, has a strong temperature dependence. In ^{1}H NMR spectra taken at low temperatures (at 77−123 K), the signals from both types of bridged hydroxyl groups are clearly resolved. With increasing temperature, the peak of the second type of bridged hydroxyl group in ^{1}H NMR spectrum broadens and its intensity decreases with the increase in the peak of the first type of bridged hydroxyl group.[4] A further increase in the temperature leads to the decrease in intensity and broadening of the one remaining peak, characteristic of the first type of bridged hydroxyl group.[4,12] With increasing temperature, analogous transformations take place in infrared spectra of zeolite ZSM-5: The intensity of the broad absorption band of the hydrogen-bonded OH groups decreases and at the same time, the band of the free bridging hydroxyl groups broadens and the maximum of that band is shifted toward lower frequencies.[2,3] The changes in spectral shapes with temperature are completely reversible.

On the basis of our calculations, some refinements can be made to Freude's model describing the relations between the first and second type of bridged hydroxyl groups.[6] At lower temperatures in some crystallographic positions, the bridging hydroxyl groups can form hydrogen bonds with nearby oxygen atoms, as described in Scheme 1. With increasing temperature,

the hydrogen bonds start to break, as evidenced by the decrease in the corresponding IR and ^{1}H NMR spectral lines.[3,4] At the same time, the increase in the band of the first type of bridged hydroxyl group indicates that the second type of bridged hydroxyl group is transformed into the first type of bridged hydroxyl group. In our calculation, this is revealed in crystallographic positions Al6−O6−Si2 and Al7−O7−Si8, where both types of bridged hydroxyl groups can be formed.

With a further increase in temperature, the protons gain sufficient energy to overcome the activation barrier to move between neighboring oxygen atoms in the AlO_4 unit.[12,55,56] As a consequence, the bridged hydroxyl groups with slightly different spectroscopic properties (with different vibrational frequencies or ^{1}H NMR chemical shifts) can be formed, and this results in the increase in the width of spectral bands of the first type of bridged hydroxyl group. The shift of the IR band maximum toward lower frequencies indicates that at higher temperatures the bridged hydroxyl groups with lower vibrational frequencies dominate in the overall set of OH groups.

As mentioned previously, the probability of finding a proton attached to a certain oxygen in the AlO_4 tetrahedron depends on the deprotonation energies of the corresponding protonation centers. Our calculations show that in the case of acid sites around the aluminum located at crystallographic position T6 the proton abstraction energy is highest at the Al6−O18−Si9 site. The OH group formed in the Al6−O18−Si9 site also has a lower vibrational frequency (3588 cm^{-1}) than the free OH group formed after the hydrogen bond breaks at the Al6−O6−Si2 site (3615 cm^{-1}). The calculated difference in vibrational frequencies (27 cm^{-1}) is in good agreement with the experimentally observed red shift (20 cm^{-1}) in vibrational frequencies ongoing from 300 to 770 K.[3] This indicates that at lower temperatures (after breaking the hydrogen bond) the occupancies of protons at various oxygen sites is kinetically controlled and thermodynamic equilibrium is reached at high temperatures. Thus, in a wide temperature range when, at different temperatures, acid sites with different acid strengthes dominate among all acidic centers present, the experimentally observable mean acidity of zeolite ZSM-5 depends on the temperature.

4. Conclusions

In the current work, Brønsted acid sites in eight different crystallographic positions of the zeolite ZSM-5 were modeled by the ONIOM3(B3LYP/6-311+G**:HF/3-21G*:MNDO) method. Both types of bridged hydroxyl groups (types 1 and 2) were represented among the studied acid sites.

Our calculations show that in the case of the second type of Brønsted acid site the hydrogen of the bridged hydroxyl group forms a hydrogen bond with one of the lattice oxygen atoms. In the case of the first type of bridged hydroxyl group, the distortion of the local environment around Al indicates that hydrogen atoms in the first type of bridged hydroxyl group are also influenced by an electrostatic interaction (primarily) with nearby oxygen atoms.

The calculated ^{1}H NMR chemical shifts and stretching vibrational frequencies of bridged hydroxyl groups are in good accordance with experimental measurements, showing that the calculation method used can reproduce the properties of zeolites acid sites well. The analysis of experimental IR and ^{1}H NMR spectra in combination with current calculations suggests that the experimentally observable mean acidity of zeolite ZSM-5 is dependent on temperature.

Acknowledgment. We gratefully acknowledge the financial support of this research by the Estonian Science Foundation (grants 3361 and 5196). We also express our thanks to one of the referees for providing many useful suggestions.

References and Notes

(1) *Introduction to Zeolite Science and Practice*; Van Bekkum, H., Flanigen, E. M., Jansen, J. C., Eds.; Studies in Surface Science and Catalysis, Vol. 58; Elsevier: Amsterdam, 1991.
(2) Datka, J.; Gil, B.; Baran, P. *Microporous Mesoporous Mater.* **2003**, *58*, 291.
(3) Zholobenko, V. L.; Kustov, L. M.; Borovkov, V.Yu;. Kazansky, V. B. *Zeolites* **1988**, *8*, 175.
(4) Beck, L. B.; White, J. L.; Haw, J. F. *J. Am. Chem. Soc.* **1994**, *116*, 9657.
(5) Brunner, E.; Beck, K.; Koch, M.; Heeribout, L.; Karge, H. G. *Microporous Mater.* **1995**, *3*, 395.
(6) Freude, D. *Chem. Phys. Lett.* **1995**, *235*, 69.
(7) Brunner, E. *J. Mol. Struct.* **1995**, *355*, 61.
(8) Brunner, E. *J. Chem. Soc., Faraday. Trans.* **1990**, *86*, 3957.
(9) Freude, D.; Klinowski, J. *J. Chem. Soc., Chem. Commun.* **1988**, 1411.
(10) Hunger, M.; Freude, D.; Pfeifer, H.; Schieger, W. *Chem. Phys. Lett.* **1990**, *167*, 21.
(11) Hunger, M.; Freude, D.; Fenzke, D.; Pfeifer, H. *Chem. Phys. Lett.* **1992**, *191*, 391.
(12) Baba, T.; Komatsu, N.; Ono, Y.; Sugisawa, H. *J. Phys. Chem. B* **1998**, *102*, 804.
(13) Sauer, J.; Sierka, M. *J. Comput. Chem.* **2000**, *21*, 1470.
(14) Brändle, M.; Sauer, J. *J. Am. Chem. Soc.* **1998**, *120*, 1556.
(15) Eichler, U.; Brändle, M.; Sauer, J. *J. Phys. Chem. B* **1997**, *101*, 10035.
(16) De Vries, A. H.; Sherwood, P.; Collins, S. J.; Rigby, A. M.; Rigutto, M.; Kramer, G. J. *J. Phys. Chem. B* **1999**, *103*, 6133.
(17) Sauer, J.; Ugliengo, P.; Garrone, E.; Saunders, V. R. *Chem. Rev.* **1994**, *94*, 2095.
(18) Derouane, E. G.; Fripiat, J. *Zeolites* **1985**, *5*, 167.
(19) Brand, H. V.; Curtiss, L. A.; Iton, L. E. *J. Phys. Chem.* **1992**, *96*, 7725.
(20) Brand, H. V.; Curtiss, L. A.; Iton, L. E. *J. Phys. Chem.* **1993**, *97*, 12773.
(21) Svensson, M.; Humbel, S.; Froese, R. D. J.; Matsubara, T.; Sieber, S.; Morokuma, K. *J. Phys. Chem.* **1996**, *100*, 19357.
(22) Humbel, S.; Sieber, S.; Morokuma, K. *J. Chem. Phys.* **1996**, *105*, 1959.
(23) Dapprich, S.; Komaromi, I.; Byun, K. S.; Morokuma, K.; Frisch, M. J. *J. Mol. Struct.: THEOCHEM* **1999**, *461−462*, 1.
(24) Karadakov, P. B.; Morokuma, K. *Chem. Phys. Lett.* **2000**, *317*, 589.
(25) Tschumper, G. S.; Morokuma, K. *J. Mol. Struct.: THEOCHEM* **2002**, *592*, 137.
(26) Sillar, K.; Burk, P. *J. Mol. Struct.: THEOCHEM* **2002**, *589−590*, 281.
(27) Panjan, W.; Limtrakul, J. *J. Mol. Struct.: THEOCHEM* **2003**, *654*, 35.
(28) Bobuatong, K.; Limtrakul, J. *Appl. Catal., A* **2003**, *253*, 49.
(29) Solans-Monfort, X.; Bertran, J.; Branchadell, V.; Sodupe, M. *J. Phys. Chem. B* **2002**, *106*, 10220.
(30) Damin, A.; Bonino, F.; Ricchiardi, G.; Bordiga, S.; Zecchina, A.; Lamberti, G. *J. Phys. Chem. B* **2002**, *106*, 7524.
(31) Van Koningsveld, H. *Acta Crystallogr., Sect. B* **1990**, *46*, 731.
(32) Frisch, M. J.; Trucks, G. W.; Schlegel, H. B.; Scuseria, G. E.; Robb, M. A.; Cheeseman, J. R.; Zakrzewski, V. G.; Montgomery, J. A., Jr.; Stratmann, R. E.; Burant, J. C.; Dapprich, S.; Millam, J. M.; Daniels, A. D.; Kudin, K. N.; Strain, M. C.; Farkas, O.; Tomasi, J.; Barone, V.; Cossi, M.; Cammi, R.; Mennucci, B.; Pomelli, C.; Adamo, C.; Clifford, S.; Ochterski, J.; Petersson, G. A.; Ayala, P. Y.; Cui, Q.; Morokuma, K.; Malick, D. K.; Rabuck, A. D.; Raghavachari, K.; Foresman, J. B.; Cioslowski, J.; Ortiz, J. V.; Stefanov, B. B.; Liu, G.; Liashenko, A.; Piskorz, P.; Komaromi, I.; Gomperts, R.; Martin, R. L.; Fox, D. J.; Keith, T.; Al-Laham, M. A.; Peng, C. Y.; Nanayakkara, A.; Gonzalez, C.; Challacombe, M.; Gill, P. M. W.; Johnson, B. G.; Chen, W.; Wong, M. W.; Andres, J. L.; Head-Gordon, M.; Replogle, E. S.; Pople, J. A. *Gaussian 98*, revision A.7; Gaussian, Inc.: Pittsburgh, PA, 1998.
(33) Derat, E.; Bouquant, J.; Humbel, S. *J. Mol. Struct.: THEOCHEM* **2003**, *632*, 61.
(34) Senchhenya, I. N.; Garrone, E.; Ugliengo, P. *J. Mol. Struct.: THEOCHEM* **1996**, *386*, 93.
(35) Kustov, L. K.; Borovkov, V. Yu.; Kazansky, V. B. *J. Catal.* **1981**, *72*, 149.
(36) Frash, M. V.; Makarova, M. A.; Rigby, A. M. *J. Phys. Chem. B* **1997**, *101*, 2116.
(37) Demuth, T.; Hafner, J.; Benco, L.; Toulhoat, H. *J. Phys. Chem. B* **2000**, *104*, 4593.

(38) Mix, H.; Sauer, J.; Schröder, K.-P.; Merkel, A. *Collect. Czech. Chem. Commun.* **1988**, *53*, 2191.
(39) Meijer, E. L.; van Santen, R. A.; Jansen, A. P. J. *J. Phys. Chem. A* **1999**, *103*, 2553.
(40) Bates, S.; Dwyer, J. *Chem. Phys. Lett.* **1994**, *255*, 427.
(41) Farnworth, K. J.; O'Malley, P. J. *J. Phys. Chem.* **1996**, *100*, 1814.
(42) Stave, S. S.; Nicholas, J. B. *J. Phys. Chem.* **1995**, *99*, 15046.
(43) Redondo, A.; Hay. P. J. *J. Phys. Chem.* **1993**, *97*, 11754.
(44) Koller, H.; Meijer, E. L.; van Santen, R. A. *Solid State Nucl. Magn. Reson.* **1997**, *9*, 165.
(45) Koller, H.; Engelhardt, G.; van Santen, R. A. *Top. Catal.* **1999**, *9*, 163.
(46) Datka, J.; Boczar, M.; Rymarowicz, P. *J. Catal.* **1988**, *144*, 368.
(47) Datka, J.; Gil, B.; Baran, P.; Staudte, B. *React. Kinet. Catal. Lett.* **2002**, *7*, 209.
(48) Heeribout, L.; Batamack, P.; Dorémieux-Morin, C.; Vincent, R.; Fraissard, J. *Colloids Surf., A* **1996**, *115*, 229.
(49) Heeribout, L.; Dorémieux-Morin, C.; Nogier, J.-P.; Vincent, R.; Fraissard, J. *Microporous Mesoporous Mater.* **1998**, *24*, 101.
(50) Sarv, P.; Fernandez, C.; Amoureux, J.-P.; Keskinen, K. *J. Phys. Chem.* **1996**, *100*, 19223.
(51) Zhang, W.; Bao, X.; Guo, X.; Wang, X. *Catal. Lett.* **1999**, *60*, 89.
(52) Kentgens, A. P.; Iuga, D.; Kalwei, M.; Koller, H. *J. Am. Chem. Soc.* **2001**, *123*, 2925.
(53) Hunger, M.; Freude, D.; Pfeifer, H. *J. Chem. Soc., Faraday Trans.* **1991**, *87*, 657.
(54) Pfeifer H. In *NMR Basic Principles and Progress*; Diehl, P.; Fluck, E., Günther, H., Kosfeld, R., Seelig, J., Eds.; Springer-Verlag: Berlin, 1994; Vol. 31, p 31.
(55) Sarv, P.; Tuherm, T.; Lippmaa, E.; Keskinen, K.; Root, A. *J. Phys. Chem.* **1995**, *99* 13763.
(56) Sierka, M. Sauer, J. *J. Phys. Chem. B* **2001**, *105*, 1603.